Available online at www.sciencedirect.com
ScienceDirect
Bioorganic & Medicinal Chemistry Letters 16 (2006) 5378–5383
Bioorganic & Medicinal Chemistry Letters

Aza-stilbenes as potent and selective c-RAF inhibitors

Octerloney McDonald, Karen Lackey, Ronda Davis-Ward, Edgar Wood, Vicente Samano, Patrick Maloney, Felix Deanda and Robert Hunter*

GlaxoSmithKline, Research Triangle Park, NC 27709, USA

Received 23 May 2006; revised 19 July 2006; accepted 21 July 2006
Available online 4 August 2006

Abstract—The synthesis of several novel aza-stilbene derivatives was carried out. The compounds were tested for their c-RAF enzyme inhibition. Compound **27** possesses significant potency against c-RAF and demonstrates selectivity over other protein kinases. A hypothesis for the binding mode, activity, and selectivity is proposed.

The kinome has become a widely targeted class of signaling proteins for drug intervention points due to the multitude of cellular regulatory roles protein kinases play.[1] At the basic level, all protein kinase enzymes bind a molecule of ATP and peptide substrate in order to propagate the signal cascade via transfer of the terminal phosphate group to a tyrosine or serine/threonine. Early research in the area targeted the protein substrate binding domain under the assumption that there was a greater probability for achieving selectivity.[2,3] Pioneering work on piceatannol derivatives and diversely substituted tyrphostins showed a number of very important concepts in the field of kinase inhibition.[4,5] Peptide mimics of the protein substrate proved difficult to make significantly potent as compared with ATP binding kinase activity inhibitors.[6] However, small changes in substitution patterns of non-peptide inhibitors of the protein substrate phosphorylation, especially compound variations that would normally emerge from a medicinal chemistry analog program, demonstrated interesting mechanism of inhibition changes (Fig. 1).[7] For example, polyhydroxylated styrenes **1** and stilbenes (piceatannol) were inhibitors by virtue of their ability to compete with peptide substrate in a kinase enzyme assay.[5] When the stilbene scaffold was substituted with halogens, as in **2**, the inhibition of kinase activity was competitive with ATP, suggesting a different binding interaction.[8]

In our research, we sought to use these types of small molecules as potential starting points in our effort to find diverse series to inhibit the MAPK signaling pathway since this may offer an ideal point to block cellular proliferation in cancer cells.[9] Examples of c-RAF inhibitors currently in the literature include Sorfenib (BAY-439006) and GW5074.[11,12] We began by performing a substructure search of the GlaxoSmithKline compound collection to select a few thousand compounds for screening in a kinase enzyme cascade assay that included c-RAF/MEK-1/ERK-2.[10]

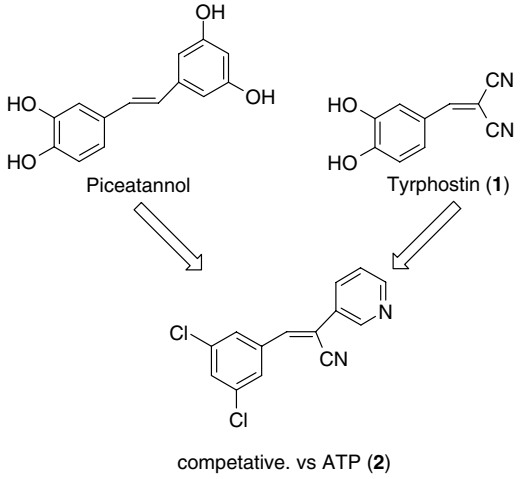

Figure 1. Historical development of modulating kinase activity via peptide substrate inhibition shifting to ATP competitive inhibition.

Keywords: Kinase; c-RAF; Aza-stilbene.
* Corresponding author. Tel.: +1 919 483 5463; e-mail: bob.n.hunter@gsk.com

0960-894X/$ - see front matter © 2006 Elsevier Ltd. All rights reserved.
doi:10.1016/j.bmcl.2006.07.063

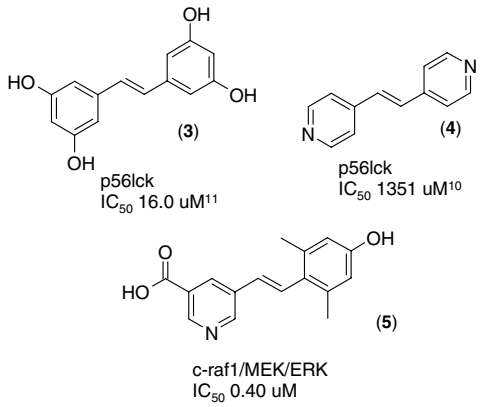

Figure 2. Related stilbene derivatives that inhibit kinase activity.

The literature examples **3** and **4** used for the basis of the substructure search are shown in Figure 2.[13,14] A very potent starting point emerged, also shown in Figure 2, which formed the basis of a lead optimization program targeting c-RAF.[15] The synthesis, highlights of the structure–activity relationships (SAR), and kinase selectivity considerations will be described.

A facile synthetic route was used to produce diversely substituted aza-stilbene analogs and is shown in Scheme 1.

The commercially available 5-bromo-nicotinonitrile, methyl 5-bromo-nicotinate, and ethyl 5-bromo-nicotinate served as good starting materials for the synthesis of the desired compounds listed in Tables 1–4. In the case of the nitrile and tetrazole containing **6**–**9**, the 5-bromo-nicotinonitrile was used in a Stille coupling with tributylvinyl tin to generate the vinyl intermediate.[16] Subsequent reaction under Heck conditions with the appropriately substituted bromo or iodo benzene gave

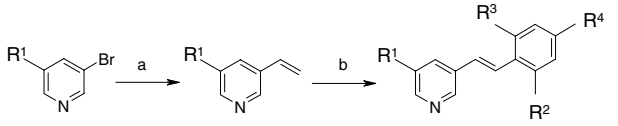

Scheme 1. Reagents and conditions: (a) tributylvinyl tin, LiCl, BHT, $Pd(PPh_3)_2Cl_2$, DMF, 70 °C; (b) arylbromide(iodide), Pd_2dba_3, TEA, P(*o*-tol)$_3$, DMF, 95 °C.

the desired aza-stilbenes in good isolated yields, generally 50 percent or better.[17] Formation of the tetrazole was accomplished with tributyl tin azide in toluene at reflux.[18] Workup of the tributyl tin azide reaction consisted of adding excess 4 M HCl in dioxane, dilution with Et_2O, and collection of the solids by vacuum filtration. Compound **10** was prepared in the same fashion from methyl 5-bromo-nicotinate (Scheme 2).

Compounds **11**–**14** were prepared from the ethyl ester by stirring the desired stilbene with 33% methyl amine or 33% dimethyl amine in EtOH at room temperature overnight. Compound **5** was prepared by the hydrolysis of **10**, and **15** was prepared by the esterification of 5-bromo nicotinic acid and subsequent Stille and Heck reactions as described above.[19]

The enzymes used in the RAF/MEK/ERK Kinase Scintillation Proximity Assay were prepared as previously described.[10] Standard compound screening assays were performed in 96-well microtiter Optiplates (Packard Instrument Co., Meriden, CT) where the final assay volume was 45 μl. Test compound (15 μl) dissolved in 6% DMSO was added to the wells followed by substrate solution (15 μl). The final assay concentrations of the reagents contained in the substrate solution were 10 μM ATP, 10 mM $MgCl_2$, 2 μM peptide substrate, biotin-AAATGPLSPGPFA, and 0.125 μCi [γ-^{33}P]ATP/well, 50 mM Mops, pH 7.6. The reactions were initiated by the addition of enzyme solution (15 μl). The final assay concentrations of the enzymes were 10 nM c-RAF1, 100 nM MEK1, and 300 nM ERK2. Positive control wells contained 6% DMSO with no added compound. Background control wells contained 50 mM EDTA. The reaction was allowed to proceed for 120 min at room temperature and was terminated by the addition of 200 μl PBS containing 2.5 mg/ml streptavidin-coated SPA beads (Amersham Biosciences, Piscataway, NJ), 50 μM ATP, 10 mM EDTA and 0.1% TX-100. The microtiter plates were sealed and SPA beads were allowed to settle for at least 6 h. The SPA signal was measured using a Packard Topcount 96-well plate scintillation counter (Packard Instrument Co.).

To determine pIC_{50} values, data were normalized to control values using the equation, $100 \times (U1 - C2)/(C1 - C2)$, where C1 is CPM in the absence of compound, C2 is CPM in the presence of excess EDTA,

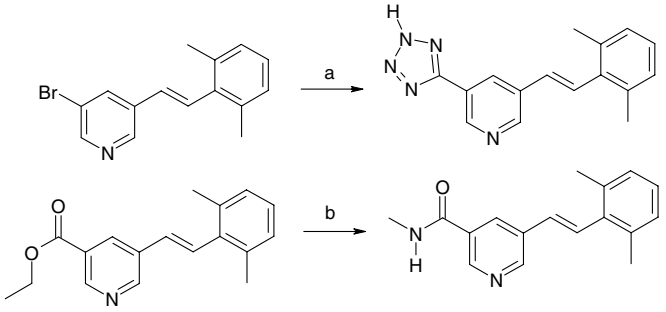

Scheme 2. Reagents and conditions: (a) tributyl tin azide, toluene, reflux; (b) 33% dimethylamine, EtOH, rt.

Table 1. c-RAF/MEK/ERK inhibition and SAR for compounds **5**–**15**

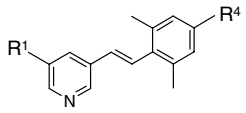

Compound	R^1	R^4	c-RAF/MEK/ERK inhibition pIC_{50}
5	COOH	OH	6.4 (0.15), $n = 4$
6	CN	OH	6.1 (0.25), $n = 4$
7	CN	H	6.0 (0.28), $n = 10$
8	Tetrazole	OH	8.4 (0.35), $n = 10$
9	Tetrazole	H	7.9 (0.3), $n = 5$
10	COOMe	OH	6.2 (0.26), $n = 3$
11	$CON(Me)_2$	OH	5.1, $n = 1$
12	CONHMe	OH	6.6 (0.15), $n = 4$
13	CONHMe	H	6.6 (0.52), $n = 4$
14	$CONH_2$	OH	6.8 (0.23), $n = 4$
15	*t*-Butyl ester	OH	5.4, $n = 1$

Standard deviation is given in parentheses. *n* values are as shown (*n* = replicates).

Table 2. c-RAF/MEK/ERK inhibition data SAR for compounds **16**–**20**

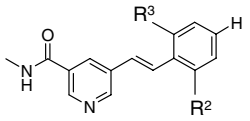

Compound	R^2	R^3	c-RAF/MEK/ERK inhibition pIC_{50}
13	CH_3	CH_3	6.6 (0.52), $n = 4$
16	CH_2CH_3	CH_2CH_3	4.6, $n = 1$
17	Cl	Cl	6.6 (0.46), $n = 4$
18	CH_3	H	5.5, $n = 1$
19	Cl	H	5.7, $n = 1$
20	CH_3	Cl	7.1 (0.56), $n = 4$

Standard deviation is given in parentheses. *n* values are as shown (*n* = replicates).

Table 3. c-RAF/MEK/ERK inhibition data SAR for compounds **21**–**27**

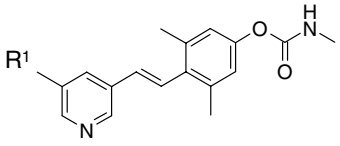

Compound	R^1	c-RAF/MEK/ERK inhibition pIC_{50}
21	CN	7.4 (0.1), $n = 3$
22	$CON(Me)_2$	5.1, $n = 1$
23	CONHMe	8.0 (0.22), $n = 4$
24	$CONH_2$	8.1 (0.18), $n = 4$
25	COOMe	7.5 (0.53), $n = 4$
26	*t*-Butyl ester	7.0 (0.33), $n = 3$
27	COOH	8.2 (0.09) $n = 3$

Standard deviation is given in parentheses. *n* values are as shown (*n* = replicates).

Table 4. c-RAF/MEK/ERK inhibition data SAR for compounds **28**–**32**

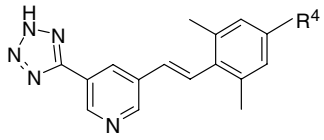

Compound	R^4	c-RAF/MEK/ERK inhibition pIC_{50}
28	2-Furan	6.2 (0.28), $n = 3$
29	2-Thiophene	6.5 (0.32), $n = 3$
30	2-Pyridyl	7.0 (0.63), $n = 4$
31	3-Thiophene	6.0, $n = 1$
32	3-Pyridyl	6.2 (0.25), $n = 2$

Standard deviation is given in parentheses. *n* values are as shown (*n* = replicates).

and U is CPM in the presence of compound. Compounds were serially diluted 3-fold and added to the reaction mixture to produce an 11-point dose–response curve ranging from 0.0001 to 10 μM. IC_{50} values were estimated using the equation $Y = V_{max} \times (1 - (X/(IC_{50} + X)))$ where Y is rate of product formation, V_{max} is the rate of the reaction in the absence of an inhibitor, and X is the inhibitor concentration. The IC_{50} value was then converted to a pIC_{50}.

Based on initial observations of the SAR, the aza-stilbene core with the ortho di-methyl groups was retained to achieve potent c-RAF inhibition. The data in Table 1 show that residues in the R^1 position which contain a hydrogen-bond acceptor/donor such as the acid, amide, or tetrazole are generally more potent in the c-RAF/MEK/ERK enzyme assay. Removal of the hydroxyl group at R^4 had very little effect on the enzyme potency.

Structure–activity relationships generated via the initial screening set suggested di-substitution ortho to the stilbene was important for enzyme activity. Maintaining a hydrogen in the 4-position of the pendant phenyl ring and the *N*-methyl amide on the pyridyl ring, Table 2, we synthesized a set of stilbenes to probe the SAR in this region. The diethyl substitution **16** was 100-fold less active than the parent, indicating a size restriction. Replacement of the methyl groups by chlorines, **17**, resulted in a compound that was equipotent with **13** in the enzyme assay. Removal of one of the methyl or chloro groups, **18** and **19**, proved to be 10-fold less active than the parent **13**. Interestingly, when only one of methyl groups was replaced with chlorine, as in **20**, the activity was increased by about 3-fold.

Placement of a *N*-methyl carbamate in the 4-position of the pendant phenyl ring, **21**–**27** in Table 3, was accomplished by reaction of the compounds where R^4 is OH in Table 1 with methylisocyanate in DMF. Incorporation of the carbamate increased enzyme potency by a minimum of 15-fold in **21** and a maximum of 60-fold in **27**.[23]

Consideration of kinase selectivity is important due to the similarities of the ATP-binding pockets of

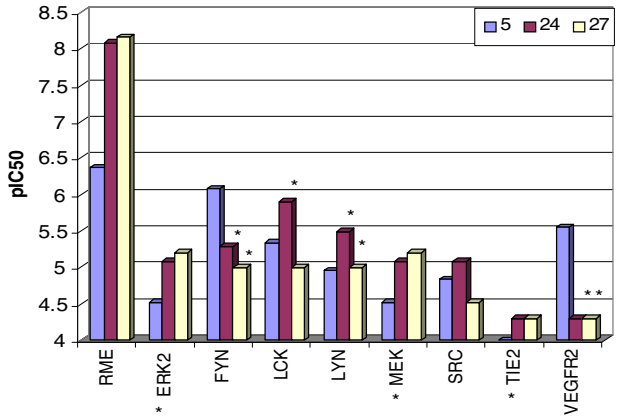

Figure 3. (*) < Value at maximum concentration tested (10 μM) also inactive on JNK3 and P38. RME = RAF-MEK-ERK,[10] FYN (mouse), LCK (mouse).

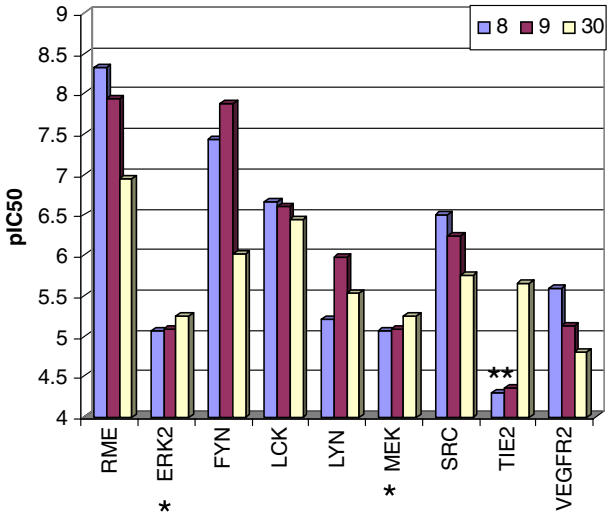

Figure 4. (*) < Value at maximum concentration tested (10 μM) also inactive on JNK3 and P38. RMK = RAF-MEK-ERK,[10] FYN (mouse), LCK (mouse).

protein kinases. As shown in Figure 3, the incorporation of the carbamate group yielded potent compounds, and it resulted in compounds that were quite selective over other representative kinases in the screening panel.

Unfortunately, the combination of both the tetrazole and the carbamate functionalities in the same molecule was not explored due to the instability of the carbamate (ex vivo studies in both mouse and human plasma demonstrated the carbamate exhibited rapid biphasic degradation to the parent phenol).[24] We instead focused on the preparation of compounds which contained the tetrazole and potential replacements for the carbamate. To do this, we prepared the triflate of **6** and used it in a second Stille reaction.[20] Listed in Table 4 are examples of the compounds prepared.

Replacement of the carbamate with a 2-pyridyl ring, **30**, resulted in only a modest loss of c-RAF activity as compared to **8** and **9**. However, this modification introduces some kinase selectivity challenges because it demonstrates activity on the SRC kinase family (FYN, LCK, LYN, and SRC).

In efforts to explain the observed c-RAF SAR and selectivity in terms of protein–ligand binding, a homology model of c-RAF was constructed from available b-RAF crystallographic data.[11] The sequence identity across their kinase domains was roughly 80% with no residue differences in their ATP-binding sites. The c-RAF model was constructed using MVP,[21] and then geometry optimized in Insight's Discover module.[22]

Designating compound **5** as the parent, substitution of the carboxylate with tetrazole resulted in a 100-fold increase in c-RAF inhibitory activity, Table 1. From Figures 3 and 4, note that this substitution also led to an increase in potency of 1.30–1.60 log units against FYN, LCK, and SRC. Such dramatic changes in activity were not observed from the two functional groups used at the R^4 position. Indeed, only **8** and **9** demonstrated a change in activity at all, where substitution of the hydroxyl with a hydrogen atom resulted in a modest 3-fold decrease in c-RAF inhibitory activity. To possibly explain why tetrazole led to an increase in potency, models of **5** and **8** in complex with c-RAF were constructed.

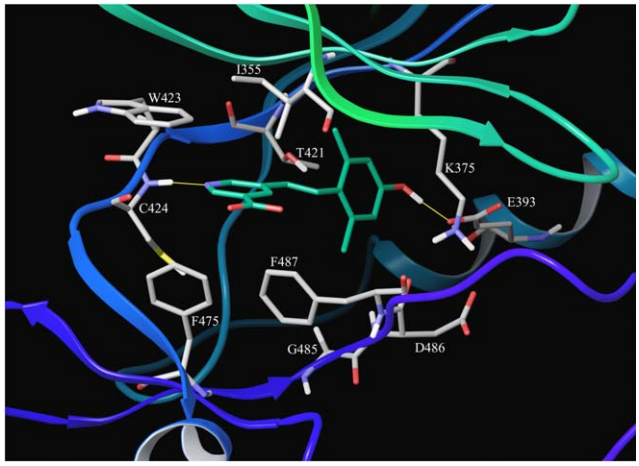

Figure 5. Structural model of c-RAF (carbon atoms in gray) in complex with compound **5** (carbon atoms in green). H-bond interactions are designated by thin yellow lines.

Illustrated in Figure 5 is a docking model of **5** in complex with c-RAF. Note that the inhibitor's pyridyl ring binds to the kinase at the hinge region with its nitrogen atom forming an H-bond interaction with the backbone NH of Cys424. The 4-hydroxy-2,6-dimethylphenyl moiety is positioned deep into the ATP-binding pocket toward the αC helix and is surrounded by mostly hydrophobic residues including Val363, Ala373, Leu397, Leu406, Ile419, and Phe487. One face of the phenyl ring makes van der Waals contact with the alkyl portion of Lys375's side chain, while the other interacts with the

side chain of Thr421. The ligand's hydroxyl is positioned toward Glu393 forming an H-bond interaction. At the opposite end of the molecule, the carboxylate is positioned at the entrance of the ATP-binding site near the protein–solvent interface where it makes van der Waals contact with three hydrophobic residues, Ile355, Phe475, and Phe487.

From Figure 6, note that the binding mode for **8** is nearly identical to that of **5**, with the difference being the tetrazole. However, given that tetrazole is significantly more lipophilic than the carboxylate, it is reasonable to conclude that **8** will have a more favorable hydrophobic interaction with Ile355, Phe475, and Phe487. Not only does the tetrazole interact more favorably with these residues, but it also makes van der Waals contact with a fourth hydrophobic residue, Trp423. Given these observations, it is apparent why the tetrazole analogues **8** and **9** are significantly more potent than the other aza-stilbene derivatives from Table 1.

Recall that substitution of the carboxylate with tetrazole also led to an increase in potency of 1.30–1.60 log units against FYN, LCK, and SRC. From our sequence analyses and superposition of LCK and SRC X-ray structures onto c-RAF, it was discovered that the four c-RAF hydrophobic residues predicted to interact with **8** corresponded to hydrophobic residues in FYN, LCK, and SRC, suggesting that the increase in potency for these other kinases was related to favorable hydrophobic interactions. In FYN, these residues are Leu277, Tyr344, Leu397, and Phe409. For LCK and SRC, the residues are Leu238, Tyr305, Leu353, Phe370 and Leu282, Tyr349, Leu402, Phe414, respectively.

Replacement of the hydroxyl at the R^4 position with *N*-methyl carbamate resulted in significant increases in c-RAF inhibitory activities, Table 3. Consider as an example **27**, which had an increase in c-RAF inhibitory activity comparable to that seen with **8**. Moreover and perhaps more importantly, **27** proved to be selective for c-RAF ($pIC_{50} = 8.16$) over the other kinases ($pIC_{50} < 5.0$) in the screening panel, Figure 3.

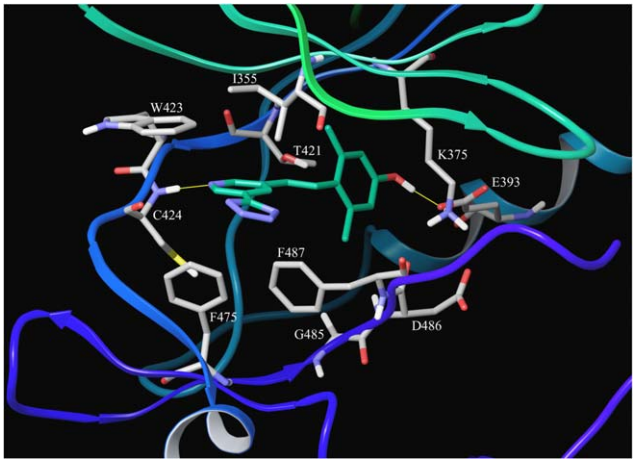

Figure 6. Structural model of c-RAF (carbon atoms in gray) in complex with compound **8** (carbon atoms in green). H-bond interactions are designated by thin yellow lines.

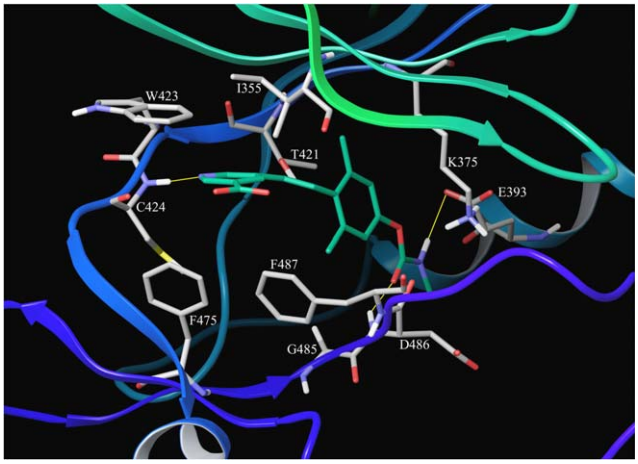

Figure 7. Structural model of c-RAF (carbon atoms in gray) in complex with compound **27** (carbon atoms in green). H-bond interactions are designated by thin yellow lines.

Illustrated in Figure 7 is a docking model of compound **27** in complex with c-RAF. The inhibitor's binding mode is similar to that already described for compounds **5** and **8**. However, compound **27** forms one additional H-bond with c-RAF. Similar to **5** and **8**, this inhibitor forms an H-bond interaction with the side chain of Glu393 through the carbamate NH. The additional H-bond interaction is formed between the inhibitor's carbonyl and the backbone NH of Asp486. We hypothesize that the increase in enzyme potency for **21**–**27** may result in part from this additional H-bond interaction with c-RAF. Note that the residue which immediately precedes Asp486 is Gly485. Based on our docking model, it is evident that formation of the H-bond interaction between the inhibitor's carbonyl and Asp486 is not sterically hindered by this glycine. However, if this residue were mutated to a larger amino acid, even one the size of alanine, the increase in side-chain volume may perhaps be sufficient to hinder the formation of this H-bond. This in turn may affect the formation of the H-bond between the carbamate NH and the glutamate (which is present in all seven kinases). In FYN, LCK, LYN, SRC, and TIE2, the residue which corresponds to Gly485 in c-Raf is an alanine. For VEGFR2, that residue is a cysteine. We hypothesize that the observed c-Raf selectivity may result in part over the ability of these non-glycine residues to sterically hinder formation of the specified H-bond interaction.

From a Piceatannol and Tyrphostin substructure search of the GSK compound collection, an aza-stilbene series was identified (**5**) for a c-RAF lead optimization effort (IC_{50} value 0.4 μM). The most potent c-RAF compound was 3,5-dimethyl-4-{(*E*)-2-[5-(1*H*-tetrazol-5-yl)-3-pyridinyl]ethenyl}phenol (**8**, IC_{50} value 0.004 μM), and it also inhibited SRC family kinases (e.g., IC_{50} value for FYN 0.040 μM). 4-{(*E*)-2-[5-(aminocarbonyl)-3-pyridinyl]ethenyl}-3,5-dimethylphenyl methylcarbamate (**25**) and 5-[(*E*)-2-(2,6-dimethyl-4-{[(methylamino)carbonyl]oxy}phenyl)ethenyl]-3-pyridinecarboxylic acid (**27**) were the most potent and selective c-RAF inhibitors synthesized. SAR was established for enhancing c-RAF potency and

selectivity, and can be explained using a homology model of c-RAF.

References and notes

1. ter Haar, E.; Walters, W. P.; Pazhanisamy, S.; Taslimi, P.; Pierce, A. C.; Bemis, G. W.; Salituro, F. G.; Harbeson, S. L. *Mini-Rev. Med. Chem.* **2004**, *4*, 235.
2. Taffs, R. E.; Sitkovsky, M. V. *J. Pharm. Sci.* **1992**, *81*, 37.
3. Saperstein, R.; Vicario, P. P.; Strout, H. V.; Brady, E.; Slater, E. E.; Greenlee, W. J.; Ondeyka, D. L.; Patchett, A. A.; Hangauer, D. G. *Biochemistry* **1989**, *28*, 5694.
4. Geahlen, R. L.; McLaughlin, J. L. *Biochem. Biophys. Res. Commun.* **1989**, *165*, 241.
5. Gazit, A.; Yaish, P.; Gilon, C.; Levitzki, A. *J. Med. Chem.* **1989**, *32*, 2344.
6. Dobrusin, E. M.; McNamara, D. J.; Fry, D. W.; Singh, J. PCT Int. Appl. WO 9411392; *Chem. Abstr*. **1994**, *121*, 173953.
7. Levitzki, A.; Gazit, A.; Osherov, N.; Posner, I.; Gilon, C. *Methods Enzymol.* **1991**, *201*, 347, *(Protein Phosphorylation, pt B)*.
8. Posner, I.; Engel, M.; Gazit, A.; Levitzki, A. *Mol. Pharmacol.* **1994**, *45*, 673.
9. Berger, D. M.; Mallon, R. *Drugs Future* **2003**, *28*, 1211.
10. McDonald, O. B.; Chen, W. J.; Ellis, B.; Hoffman, C.; Overton, L.; Rink, M.; Smith, A.; Marshall, C. J.; Wood, E. R. *Anal. Biochem.* **1999**, *268*, 318.
11. Wan, P. T. C.; Garnett, M. J.; Roe, S. M.; Lee, S.; Niculescu-Duvaz, D.; Good, V. M.; Cancer Genome Project; Jones, C. M.; Marshall, C. J.; Springer, C. J. et al. *Cell* **2004**, *116*, 855 (PDB code 1UWH).
12. Compound **1**: Lackey, K.; Cory, M.; Davis, R.; Frye, S. V.; Harris, P. A.; Hunter, R. N.; Jung, D. K.; McDonald, O. B.; McNutt, R. W.; Peel, M. R.; Rutkowske, R. D.; Veal, J. M.; Wood, E. R. *Bioorg. Med. Chem. Lett.* **2000**, *10*, 223.
13. Cushman, M.; Nagarathnam, D.; Gopal, D.; Geahlen, R. L. *Bioorg. Med. Chem. Lett.* **1991**, *1*, 211.
14. Thakkar, K.; Geahlen, R. L.; Cushman, M. *J. Med. Chem.* **1993**, *36*, 2950.
15. Maloney, P. R.; Parks, D. J.; Haffner, C. D.; Fivush, A. M.; Chandra, G.; Plunket, K. D.; Creech, K. L.; Moore, L. B.; Wilson, J. G.; Lewis, M. C.; Jones, S. A.; Willson, T. M. *J. Med. Chem.* **2000**, *43*, 2971.
16. Farina, V.; Krishnamurphy, V.; Scott, W. J. *Org. React.* **1997**, *50*, 1 (review).
17. Heck, R. F. *Palladium Reagents in Organic Synthesis*; Academic Press LTD: London, 1985.
18. Thomas, A. P.; Allott, C. P.; Gibson, K. H.; Major, J. S.; Masek, B. B.; Oldham, A. A.; Ratcliffe, A. H.; Roberts, D. A.; Russell, S. T.; Thomason, D. A. *J. Med. Chem.* **1992**, *35*, 877.
19. Widmer, U. *Synthesis* **1983**, 135.
20. Stille, J. K.; Echavarren, A. M. *J. Am. Chem. Soc.* **1987**, *109*, 5478.
21. Millard, H. L. Docking Conformationally Flexible Molecules into Protein Binding Sites. In *Practical Application of Computer-Aided Drug Design*; Charifson, P. S., Ed.; Marcel Dekker, 1997; p 243.
22. *Insight II Molecular Modeling System*, Version 2005, Accelrys, Inc., San Diego, CA, 2005.
23. Analytical data for **27**, 1H NMR (300 MHz, DMSO-d_6) δ ppm 2.3 (s, 6H) 2.6 (d, J = 4.6 Hz, 3H) 6.8 (m, 3H) 7.5 (d, J = 16.6 Hz, 1H) 7.6 (q, J = 4.7 Hz, 1H) 8.5 (t, J = 1.9 Hz, 1H) 9.0 (d, J = 1.9 Hz, 1H) 9.0 (d, J = 2.1 Hz, 1H), LCMS m/z: 325 $[M-H]^-$.
24. Data unpublished.